

# Theory of angular magnetoresistance oscillations in $\text{Tl}_2\text{Ba}_2\text{CuO}_6$

Adrian Drăgulescu and Victor M. Yakovenko

Department of Physics and Center for Superconductivity Research, University of Maryland, College Park, Maryland 20742

David J. Singh

Complex Systems Theory Branch, Naval Research Laboratory, Washington DC 20375  
(cond-mat/9811101, v.1: November 6, 1998, v.2: March 28, 1999)

Using the calculated electron energy band structure of  $\text{Tl}_2\text{Ba}_2\text{CuO}_6$ , we compute the dependence of the  $\mathbf{c}$  axis magnetoresistance on the orientation of the magnetic field for different magnitudes of the magnetic field. We explain the known experimental results for the in-plane rotation of the magnetic field and predict the shape of the magnetoresistance oscillations for the out-of-plane rotations of the magnetic field. We show how the latter oscillations can be utilized to reconstruct the shape of the Fermi surface and to study the coherence of interplane electron tunneling.

PACS Numbers: 74.72.Fq, 72.15.Gd

In a strong magnetic field, the electrical resistivity of a layered metal oscillates when the magnetic field is rotated between the orientations perpendicular and parallel to the layers. This effect, called the angular magnetoresistance oscillations (AMRO), was originally discovered in the layered organic conductors of the BEDT-TTF family (see review [1]) and remains largely unknown outside of the organic conductors research community. AMRO should not be confused with the Shubnikov-de Haas magnetoresistance oscillations, which occur when the *magnitude*, not the *orientation*, of the magnetic field is changed. Using AMRO it is possible to determine not only the area, but also the shape of the Fermi surface of a layered metal [2]. It would be very interesting to observe AMRO experimentally in the high- $T_c$  superconductors, which are also layered materials. That would provide information about the structure of their Fermi surfaces and the coherence of interlayer electron motion.

In this paper, we calculate the dependence of the  $\mathbf{c}$ -axis (interlayer) electrical resistivity of  $\text{Tl}_2\text{Ba}_2\text{CuO}_6$  on the orientation of a magnetic field and obtain detailed AMRO curves for comparison with the past and future experiments [3]. The greater the value of  $\omega_c\tau$ , where  $\omega_c$  is the cyclotron frequency and  $\tau$  is the electron scattering time, the more pronounced AMRO are. We believe that  $\text{Tl}_2\text{Ba}_2\text{CuO}_6$  is one of the best candidates for the experimental observation of AMRO because a relatively high value  $\omega_c\tau = 0.9$  has been recently achieved in this material using a pulsed magnetic field of 60 T [4]. Moreover, AMRO for the magnetic field rotation within the most conducting ( $\mathbf{a}, \mathbf{b}$ ) plane have been already observed experimentally in this material at the field of 13 T and  $\omega_c\tau = 0.16 \div 0.31$  [5].

$\text{Tl}_2\text{Ba}_2\text{CuO}_6$  has the body-centered tetragonal crystal structure with in-plane lattice spacings  $a = b = 3.6 \text{ \AA}$  and the distance  $d = 11 \text{ \AA}$  between the  $\text{CuO}_2$  planes. The electron band structure of  $\text{Tl}_2\text{Ba}_2\text{CuO}_6$  has been calculated in Ref. [6]. Two energy bands cross the Fermi

level: the Cu-O hole band centered at the Brillouin zone corner X and the Tl-O electron band centered at  $\Gamma$ . The Tl-O Fermi surface is a closed spheroid, which does not contribute significantly to the conductivity, so it will be ignored in our calculations. The Cu-O band is the generic band of the layered high- $T_c$  cuprates. Its Fermi surface has the shape of a slightly corrugated cylinder, open along the  $\mathbf{c}$  direction. The electron dispersion law is a sum of the in-plane and interplane terms:

$$\epsilon(k_x, k_y, k_z) = \epsilon_{\parallel}(k_x, k_y) + \epsilon_{\perp}(k_x, k_y, k_z), \quad (1)$$

where  $\epsilon$  is the electron energy, and  $k_x$ ,  $k_y$ , and  $k_z$  are the electron wave vectors along the  $\mathbf{a}$ ,  $\mathbf{b}$ , and  $\mathbf{c}$  axes. The in-plane dispersion law  $\epsilon_{\parallel}(k_x, k_y)$  has been calculated numerically in Ref. [6] on a mesh of  $32 \times 32$  points and interpolated in between. For the interplane dispersion law  $\epsilon_{\perp}(k_x, k_y, k_z)$ , we select the tight-binding one, in accordance with the body-centered unit cell:

$$\epsilon_{\perp} = -8t_{\perp} \cos(k_x a/2) \cos(k_y b/2) \cos(k_z d), \quad (2)$$

where the interplane electron tunneling amplitude  $t_{\perp}$  is much smaller than the Fermi energy  $E_F$ .

The orientation of the magnetic field  $\mathbf{H}$  is characterized by the polar angle  $\theta$  relative to the  $\mathbf{c}$  ( $z$ ) axis perpendicular to the layers and the azimuthal angle  $\phi$  relative to the  $\mathbf{a}$  ( $x$ ) axis parallel to the Cu-O bonds. Within a semiclassical picture, the electron wave vector  $\mathbf{k}$  changes in time  $t$  according to the Lorentz equation of motion:

$$d\mathbf{k}/dt = (e/\hbar c) \mathbf{v} \times \mathbf{H}, \quad \text{where } \mathbf{v} = \partial\epsilon/\hbar\partial\mathbf{k}. \quad (3)$$

Here  $e$  is the electron charge,  $c$  is the speed of light, and  $\hbar$  is the Planck constant.

The interplane component of the electrical conductivity tensor  $\sigma_{zz}$ , obtained by solving the linearized Boltzmann equation in the  $\tau$  approximation, is given the Shockley-Chambers formula [7]:

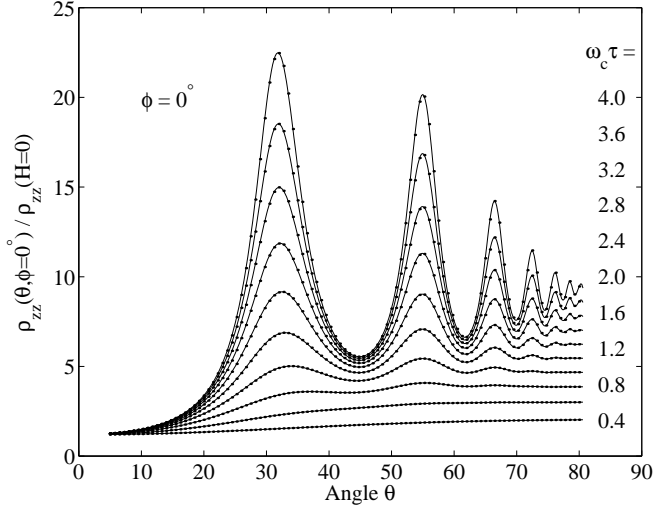


FIG. 1. Angular oscillations of  $\rho_{zz}$  vs  $\theta$  for  $\phi = 0^\circ$  at different values of  $\omega_c \tau$ .

$$\sigma_{zz} = 2e^2 \int \frac{d^3 k(0)}{(2\pi)^3} \left( -\frac{\partial f}{\partial \epsilon} \right) v_z[\mathbf{k}(0)] \times \int_0^\infty dt v_z[\mathbf{k}(t)] e^{-t/\tau}. \quad (4)$$

In Eq. (4),  $f$  is the Fermi distribution function,  $\tau$  is the electron scattering time, and the first integral is taken over the electron wave vector  $\mathbf{k}(0)$  that serves as the initial condition for determining  $\mathbf{k}(t)$  from the Lorentz equation of motion (3).

When  $\theta \neq 0$ , electrons circle around the Fermi surface along the closed orbits obtained by cutting the Fermi surface with the planes perpendicular to the magnetic field. The different planes are labeled by the component  $k_H$  of the electron wave vector parallel to the magnetic field. In this case, Eq. (4) can be rewritten as

$$\sigma_{zz} = \frac{e^3 H}{4\pi^3 \hbar^2 c} \frac{1}{1 - \exp(-T/\tau)} \times \int dk_H \int_0^T dt v_z[\mathbf{k}(t)] \int_0^T dt' v_z[\mathbf{k}(t-t')] e^{-t'/\tau}, \quad (5)$$

where  $T$  is the period of electron motion.

Because  $t_\perp/E_F$  is very small, we neglect  $v_z$  in Eq. (3), which then reduces to the in-plane equations of motion for  $k_x(t)$  and  $k_y(t)$ , while  $k_z(t)$  is determined from the geometrical relation

$$k_z(t) = K_z - k_\phi(t) \tan \theta. \quad (6)$$

Here  $K_z = k_H / \cos \theta$ , and

$$k_\phi(t) = k_x(t) \cos \phi + k_y(t) \sin \phi \quad (7)$$

is the projection of the in-plane electron wave vector onto the in-plane component of the magnetic field [2].

Substituting  $v_z$  from Eq. (2) into Eq. (5), using Eq. (6), and taking the integral over  $K_z$ , we find:

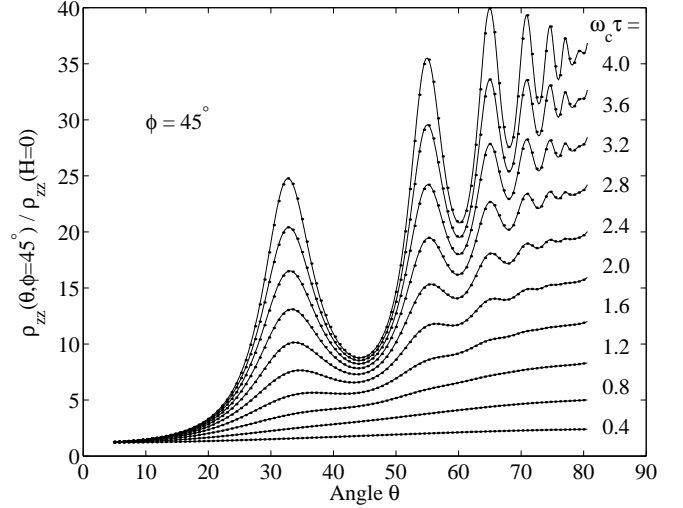


FIG. 2. Angular oscillations of  $\rho_{zz}$  vs  $\theta$  for  $\phi = 45^\circ$  at different values of  $\omega_c \tau$ .

$$\sigma_{zz}(\theta, \phi) = \frac{16e^2 m_c t_\perp^2 d}{\pi^2 \hbar^4 \omega_c \cos \theta} \frac{1}{1 - \exp(-2\pi/\omega_c \tau \cos \theta)} \times \int_0^{2\pi} d\zeta \int_0^{2\pi} d\zeta' \cos\{d[k_\phi(\zeta) - k_\phi(\zeta - \zeta')] \tan \theta\} \times \cos \frac{ak_x(\zeta)}{2} \cos \frac{ak_y(\zeta)}{2} \cos \frac{ak_x(\zeta - \zeta')}{2} \cos \frac{ak_y(\zeta - \zeta')}{2} \times \exp(-\zeta'/\omega_c \tau \cos \theta). \quad (8)$$

In Eq. (8),  $t$  has been replaced by the dimensionless variable  $\zeta = \omega_c t$ , where  $\omega_c$  is the in-plane cyclotron frequency for  $\theta = 0$ :

$$\omega_c = \frac{2\pi e H}{\hbar \oint dk_l / v} = \frac{e H}{m_c c}. \quad (9)$$

In Eq. (9), the integral is taken along the Fermi surface in the  $(k_x, k_y)$  plane, and  $m_c$  is, by definition, the cyclotron mass.

We have integrated the Lorentz equations of motion for  $k_x(t)$  and  $k_y(t)$  and evaluated the integral (8) numerically for different values of the parameter  $\omega_c \tau$  and different orientations of the magnetic field. The resultant resistivity  $\rho_{zz} = 1/\sigma_{zz}$  [8] is shown in Figs. 1, 2, and 3. For a fixed azimuthal angle  $\phi$ ,  $\rho_{zz}$  displays oscillations as a function of the polar angle  $\theta$ . Figs. 1 and 2 demonstrate that, while the amplitude of oscillations grows with increasing  $\omega_c \tau$ , the angles  $\theta_n$  where  $\rho_{zz}$  has the  $n$ -th maximum do not depend on  $\omega_c \tau$ .

The values of  $\theta_n$  can be related to the shape of the Fermi surface via the following analytical argument [2]. The maxima in  $\rho_{zz}$  become sharp in the limit  $\omega_c \tau \gg 1$ . In this limit, as follows from Eq. (5),  $\sigma_{zz} \propto \tau \langle \bar{v}_z^2 \rangle$ , where  $\langle \dots \rangle$  denotes the averaging over different electron orbits (the integration over  $k_H$ ), and

$$\bar{v}_z = \frac{8t_\perp d}{\hbar} \int_0^{2\pi} d\zeta \cos \frac{ak_x(\zeta)}{2} \cos \frac{ak_y(\zeta)}{2}$$

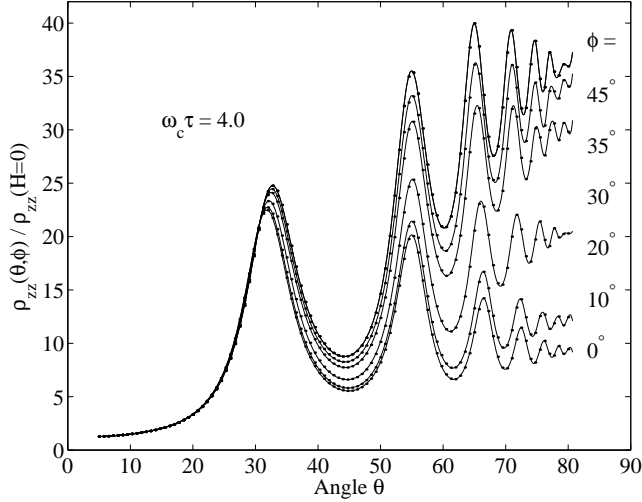


FIG. 3. Angular oscillations of  $\rho_{zz}$  vs  $\theta$  for different  $\phi$  at  $\omega_c \tau = 4.0$ . The curve for  $\phi = 40^\circ$  is the same as for  $\phi = 45^\circ$ .

$$\times \sin [K_z d - k_\phi(\zeta) d \tan \theta] \quad (10)$$

is the average of  $v_z$  along a given electron orbit. In the limit  $(d/a) \tan \theta \gg 1$ , the argument of sine in Eq. (10) oscillates very fast as a function of  $\zeta$ . Thus the integral is dominated by the points where the phase is stationary. These are the turning points of the electron trajectory, where  $k_\phi$  achieves the maximal  $k_\phi^{\max}$  and minimal  $-k_\phi^{\max}$  values. Evaluating the integral (10) asymptotically in the vicinity of the stationary points, we find [2]:

$$\bar{v}_z \propto \sin(K_z d) \cos(k_\phi^{\max} d \tan \theta - \pi/4). \quad (11)$$

When the argument of cosine in Eq. (11) is equal to  $\pi(n - 1/2)$  (where  $n = 1, 2, \dots$ ), the average electron velocity vanishes:  $\bar{v}_z = 0$ , thus  $\sigma_{zz} \rightarrow 0$  and  $\rho_{zz} \rightarrow \infty$  [9]. This situation corresponds to the resistivity maxima in Figs. 1, 2, and 3, and takes place at the angles

$$\tan \theta_n = \frac{\pi(n - 1/4)}{k_\phi^{\max} d}. \quad (12)$$

The same condition (12) follows from the derivation even if  $\tau$  varies along the Fermi surface [10].

Eq. (12) shows that  $\tan \theta_n$  increases linearly with the maximum number  $n$ , and the slope of this dependence is determined by  $k_\phi^{\max}$ . In Fig. 3, we plot  $\rho_{zz}$  vs  $\theta$  for different  $\phi$ . For each curve, we determine the angles of the resistivity maxima  $\theta_n$  and plot  $\tan \theta_n$  vs  $n$  in Fig. 4. Using Eq. (12), we determine  $k_\phi^{\max}$  from the slopes of the lines in Fig. 4 and plot  $k_\phi^{\max}$  vs  $\phi$  in Fig. 5 as the black dots. To reconstruct the Fermi surface, it is necessary to draw a line through each black dot in Fig. 5 perpendicular to the vector  $\mathbf{k}_\phi^{\max}$ . The envelope of these lines gives the Fermi surface [2]. One can check in Fig. 5 that this procedure indeed reproduces the actual Fermi surface of our model [6], which is shown by the solid line.

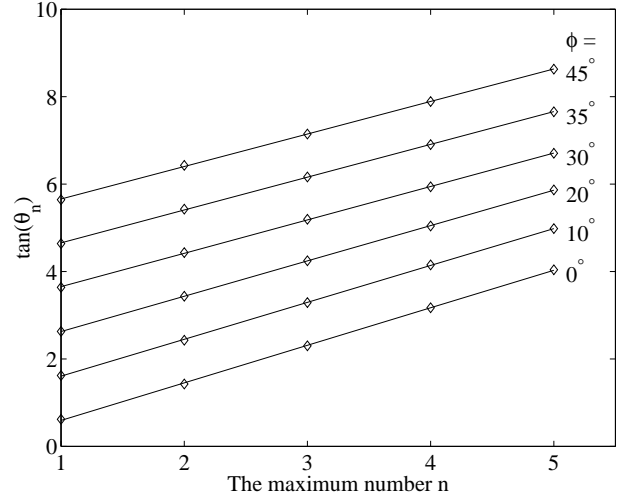


FIG. 4. The linear dependence of  $\tan \theta_n$  vs the maximum number  $n$ . The lines are offset vertically for different  $\phi$ .

Thus, measuring AMRO in  $\text{Tl}_2\text{Ba}_2\text{CuO}_6$  experimentally for every angle  $\phi$  and applying the described above procedure, one could reconstruct the in-plane shape of the Fermi surface in this material.

Now, let us discuss AMRO of  $\rho_{zz}$  vs  $\phi$  for the magnetic field rotation within the  $(x, y)$  plane at  $\theta = 90^\circ$ . In this case, the electron orbits are open along the  $\mathbf{c}$  axis. Neglecting  $v_z$  in Eq. (3), we find that only  $k_z$  depends on time:  $k_z(t) = k_z(0) - (eH/c\hbar)(v_x \sin \phi - v_y \cos \phi)t$ . Neglecting  $\epsilon_\perp$  in Eq. (1), we can write the volume of integration in Eq. (4) as  $d^3 k(0) = dk_z(0) d\epsilon_\parallel dk_l / \hbar v$ , where the differential  $dk_l$  is taken along the Fermi surface in the  $(k_x, k_y)$  plane. Substituting  $v_z$  from Eq. (2) into Eq. (4), using  $k_z(t)$ , and taking the integrals over  $\epsilon_\parallel$ ,  $k_z(0)$ , and  $t$ , we find:

$$\sigma_{zz}(90^\circ, \phi) = \frac{8e^2 t^2 \tau d}{\pi^2 \hbar^3} \int \frac{dk_l}{v} \frac{\cos^2 \frac{ak_x}{2} \cos^2 \frac{ak_y}{2}}{1 + [\omega_z(\phi)\tau]^2}. \quad (13)$$

In Eq. (13),

$$\omega_z(\phi) = \frac{ed}{\hbar c} |\mathbf{v} \times \mathbf{H}| = \frac{edH}{\hbar c} |v_x \sin \phi - v_y \cos \phi| \quad (14)$$

is the frequency of the electron motion across the Brillouin zone in the  $k_z$  direction. Similar equations were obtained in Ref. [11].

Using Eq. (13), we have numerically calculated  $\rho_{zz}(90^\circ, \phi)$  and plotted it in Fig. 6 for different values of  $\omega_c \tau$ . One can see that  $\rho_{zz}$  is minimal at  $\phi = 0^\circ$  and maximal at  $\phi = 45^\circ$ . This result is in agreement with Fig. 3 and with the experiment [5]. This behavior can be qualitatively understood in the following way. According to Eqs. (13) and (14),  $\sigma_{zz}(90^\circ, \phi)$  is dominated by the regions of the Fermi surface where  $\omega_z(\phi)$  is minimal, that is where  $\mathbf{v}$  is parallel to  $\mathbf{H}$  [11]. When the magnetic field points along the  $x$  axis, these regions are relatively

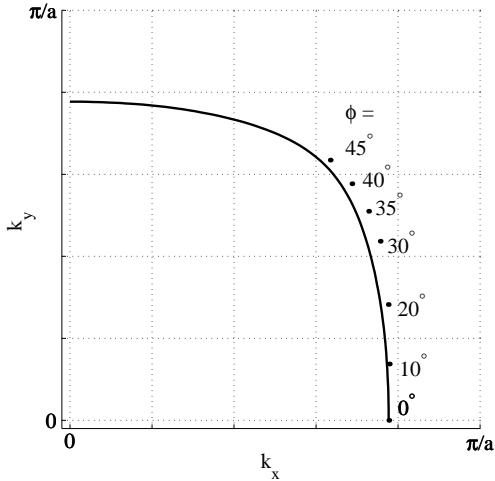


FIG. 5. Dots:  $\mathbf{k}_\phi^{\max}$  vs  $\phi$ . Solid line: The Fermi surface of  $\text{Tl}_2\text{Ba}_2\text{CuO}_6$ . The normals to the radii defined by the dots and drawn through the dots envelope the Fermi surface.

flat and large (see Fig. 5). On the other hand, when the magnetic field points at  $45^\circ$  to the  $x$  axis, these regions are curved and relatively small. Thus, the conductivity is higher when  $\mathbf{H}$  is parallel to  $x$  [12].

The experiment [5] was actually performed in the regime  $\omega_c\tau \ll 1$ . In this case,  $\rho_{zz}$  can be expanded in the powers of the magnetic field  $H$ :  $\rho_{zz} = \rho_{zz}^{(0)} + \Delta\rho_{zz}^{(2)} - \Delta\rho_{zz}^{(4)}$ , where  $\rho_{zz}^{(0)}$  is the zero-field resistance, and  $\Delta\rho_{zz}^{(2)}$  and  $\Delta\rho_{zz}^{(4)}$  are the positive terms proportional to  $H^2$  and  $H^4$ , respectively. Angular dependence appears only in the  $\Delta\rho_{zz}^{(4)}$  term, which can be written as  $\Delta\rho_{zz}^{(4)} = \bar{\rho}_{zz}^{(4)} + \tilde{\rho}_{zz}^{(4)} \cos(4\phi)$ . Expanding Eq. (13) in the powers of  $\omega_c\tau$  and calculating the integrals numerically, we find the value 0.505 for the dimensionless ratio  $\tilde{\rho}_{zz}^{(4)}\rho_{zz}^{(0)}/[\Delta\rho_{zz}^{(2)}]^2$ , which does not depend on the magnetic field and the scattering time  $\tau$ . This value agrees with the experimentally measured one  $0.6 \pm 0.1$  [5]. We also obtain the value 0.16 for the dimensionless ratio of the angular-dependent and angular-independent terms  $\tilde{\rho}_{zz}^{(4)}/\bar{\rho}_{zz}^{(4)}$ . The experiment [5] finds that this ratio varies with temperature between 0.15 and 0.06. The temperature dependence may be due to different temperature dependences of  $\tau$  at the different parts of the Fermi surface [10], which is not considered in our model.

Our results are obtained from the Boltzmann equation in the lowest order in the interplane electron tunneling amplitude  $t_\perp$ , which appears only as a prefactor in Eqs. (8) and (13). Equivalent results can be obtained using the lowest-order perturbation theory in  $t_\perp$  and the in-plane electron Green functions [13]. AMRO exist both when the interplane electron motion is coherent  $t_\perp \geq \hbar/\tau$  or weakly incoherent  $t_\perp \leq \hbar/\tau$  [13]. On the other hand, if the interplane tunneling is strongly incoherent, so that electrons lose phase memory, and the in-plane electron momentum is not conserved, AMRO should not exist.

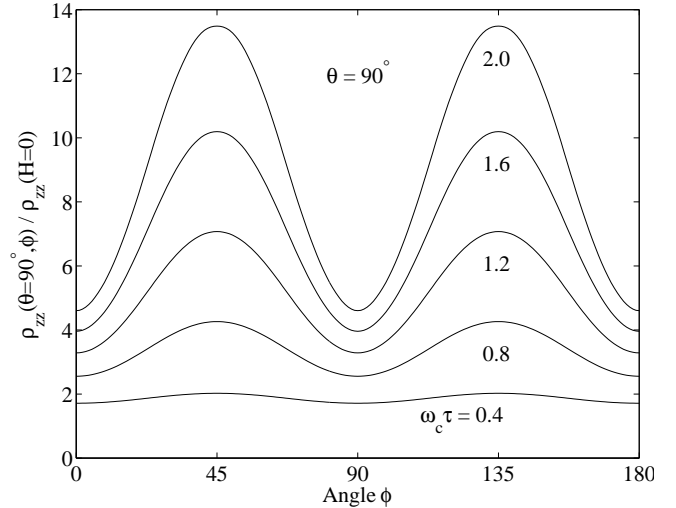


FIG. 6. Angular oscillations of  $\rho_{zz}$  vs  $\phi$  for  $\theta = 90^\circ$  at different values of  $\omega_c\tau$ .

The experimental observation of AMRO in  $\text{Tl}_2\text{Ba}_2\text{CuO}_6$  [5] indicates that the interplane tunneling in this material corresponds to the former case.

- [1] M. V. Kartsovnik and V. N. Laukhin, J. Phys. I (France) **6**, 1753 (1996).
- [2] M. V. Kartsovnik *et al.*, J. Phys. I (France), **2**, 89 (1992).
- [3] We have also calculated AMRO for  $\text{Bi}_2\text{Sr}_2\text{CaCu}_2\text{O}_8$  using the electron dispersion law determined from the photoemission experiment [14] and found results similar to those for  $\text{Tl}_2\text{Ba}_2\text{CuO}_6$ .
- [4] A. W. Tyler *et al.*, Phys. Rev. B **57**, R728 (1998).
- [5] N. E. Hussey *et al.*, Phys. Rev. Lett. **76**, 122 (1996).
- [6] D. J. Singh and W. E. Pickett, Physica C **203**, 193 (1992).
- [7] J. M. Ziman, *Principles of the Theory of Solids* (Cambridge University Press, Cambridge, 1972).
- [8] The off-diagonal components of the conductivity tensor  $\sigma_{zx}$  and  $\sigma_{zy}$ , given by equations similar to Eq. (5), vanish because of the integration of  $v_z$  over  $K_z$ , so  $\rho_{zz} = 1/\sigma_{zz}$ .
- [9] For *generic* closed orbits, one expects  $\bar{v}_z \neq 0$  and saturation of  $\rho_{zz}$  at  $\omega_c\tau \gg 1$  [7]. However,  $\bar{v}_z$  may vanish for some *special* orientations of the magnetic field given by Eq. (12).
- [10] A. T. Zheleznyak *et al.*, Phys. Rev. B **57**, 3089 (1998); **59**, 207 (1999).
- [11] A. G. Lebed and N. N. Bagmet, Phys. Rev. B **55**, R8654 (1997); A. J. Schofield, J. R. Cooper, and J. M. Wheatley, cond-mat/9709167.
- [12] L. N. Bulaevskii, M. J. Graf, and M. P. Maley (unpublished) pointed out that in the  $d$ -wave *superconducting* state the resistivity of normal quasiparticles (located near the gap nodes) should be *minimal* at  $\phi = 45^\circ$ , when the magnetic field points to the nodes. Thus, the pattern shown in Fig. 6 for the normal state should be reversed in the superconducting state.
- [13] R. H. McKenzie and P. Moses, Phys. Rev. Lett. **81**, 4492 (1998); cond-mat/9812113.
- [14] M. R. Norman *et al.*, Phys. Rev. B **52**, 615 (1995).